Radiomics Signature: A Biomarker for the Preoperative Distant Metastatic Prediction of Stage I Nonsmall Cell Lung Cancer

Li Fan[1], MengJie Fang[1], WenTing Tu[1], Di Zhang, Yun Wang, Xiuxiu Zhou, Yi Xia, ZhaoBin Li, ShiYuan Liu

Abbreviations

CEA carcinoembryonic antige

C-index concordance index

CT computed tomography

DM distant metastasis

DMFS distant metastasis free survival

HR hazard ratio

IASLC International Association for the Study of Lung Cancer

IGP intra group proportions

LASSO the least absolute shrinkage and selection operator

NSCLC nonsmall cell lung cancer

RS radiomcis signatures

TNM tumor node metastasis

Objectives: To evaluate the predictive value of radiomics features on the distant metastasis (DM) of stage I nonsmall cell lung cancer (NSCLC) preoperatively, by comparing with clinical characteristics and CT morphological features, and to screen the important prognostic predictors.

Methods: One hundred ninety-four stage I NSCLC patients were retrospectively enrolled, DM free survival (DMFS) was evaluated. The consensus clustering analysis was used to build the radiomics signatures in the primary cohort and validated in the validation cohort. The univariate survival analysis was performed in clinical characteristics, CT morphological features and radiomics signatures, respectively. Cox model was performed and C-index was calculated.

Results: There were 25 patients (12.9%) with DM. The median DMFS was 15 months. Three hundred thirteen radiomics features were selected, then classified into five groups, two subtypes (I and II) with each group. The RS1 showed the best prognostic ability with C-index of 0.355(95% confidence interval [CI], 0.269−0.442; $p < 0.001$). The histological type exhibited a good prognostic ability with C-index of 0.123 (95% CI, 0.000−0.305; $p < 0.001$) for DMFS. Cox model showed RS1(hazard ratio [HR] 18.025, 95% CI 2.366−137.340), pleural indentation sign (HR 2.623, 95% CI 1.070−6.426) and histological type (HR 4.461, 95% CI 1.783−11.162) were the independent prognostic factors ($p < 0.05$).

Conclusion: Radiomics provided a new modality for the distant metastatic prediction of stage I NSCLC. Patients with type II of RS1, pleural indentation sign and nonadenocarcinoma indicated the high probability of postsurgical DM.

Key Words: Lung; Nonsmall cell lung cancer; Tomography, X-ray computed; Computational biology; Prognosis.

Acad Radiol 2019; 26:1253−1261

From the Department of Radiology, Changzheng Hospital, Second Military Medical University, No. 415 Fengyang Road, Shanghai 200233, China (L.F., W.T., D.Z., Y.W., X.Z., Y.X., S.L.); CAS Key Laboratory of Molecular Imaging, Institute of Automation, Chinese Academy of Sciences, Beijing, China (M.F.); University of Chinese Academy of Sciences, Beijing, China (M.F.); Department of Radiation Oncology, Shanghai Jiao Tong University Affiliated Sixth People's Hospital, No. 600 Yishan Road, Shanghai 200233, China (Z.L.). Received September 24, 2018; revised October 28, 2018; accepted November 12, 2018. **Address correspondence to:** Z.B.L. and S.Y.L. e-mails: lizhaobin79@163.com, lsy0930@163.com

[1] These authors contributed equally to this work.

https://doi.org/10.1016/j.acra.2018.11.004

INTRODUCTION

Lung cancer is the leading cause of cancer-related mortality worldwide. The prognosis of lung cancer varied on different clinical overall stage. According to the eighth edition stage groups in the National Cancer Data Base (1), median overall survival in patients with nonsmall cell lung cancer (NSCLC) ranged from 103 months for the stage IA1 group to 4.9 months for the stage IV group. The stage I groups had 5-year survival rates ranging from 69% to 53%.

While the 5-year survival rate for the stage IV group was only 3%. Moreover, the overall survival of stage IA group was statistically distinct from stage IB group ($p < 0.0001$). The radical surgery is the first choice of stage I NSCLC, but there are still 30%−40% patients with recurrence and/or distant metastasis (DM) (2). The adjuvant therapy is recommended for stage IB NSCLC postsurgery, while not for stage IA NSCLC. Moreover, it has been reported that relapsed and de novo patients represent significantly different subpopulations within metastatic NSCLC with the latter exhibiting poorer survival (3). Therefore, screening the early stage NSCLC with the potential of DM is important to instruct the timely therapy, improve the survival and reduce the de novo disease. The patients with high risk of DM should receive postsurgical adjuvant therapy, not only improving the therapeutic effect, but also escaping the over-therapy for the low risk patients. Tumor node metastasis (TNM) stage is the most common modality to predict the potential survival and metastasis in clinical practice (4). However, the DM varied even for the same TNM stage patients, due to the heterogeneity of the tumor. It has been reported that CT morphological features, quantitative imaging, histogram analysis, and metabolism of PET/CT could predict the survival of lung cancer (5−8).

Radiomics is an emerging field that converts imaging data into a highdimensional mineable feature space using a large number of automatically extracted data characterization algorithms (9). It contains many potential markers for the disease occurrence, progress and prognosis, and could instruct the therapy and predict the prognosis. It has been reported that radiomics could predict the lymph node metastasis in gastric cancer, the prognosis of stage III NSCLC, and so on (10,11). The most important is that radiomics could reflect the heterogeneity of the tumor, helping for the individualized precision evaluation of the therapy. The radiomic signature associated with the predicting DM of stage I NSCLC has not yet been fully explored.

Therefore, the present study sought to evaluate the predictive value of radiomics features on the DM of stage I NSCLC preoperatively, by comparing with clinical characteristics and CT morphological features, and to screen the important prognostic predictors, instructing the individualized precision therapy.

MATERIALS AND METHODS

Patient Population

From April 2012 to February 2016, 404 consecutive patients with NSCLC confirmed by operative pathology were admitted in one hospital and included in the study for the radiomics signature building. Computer-generated random numbers were used to split 243 patients into the primary cohort (113 males and 130 females; median age 62 years old, range 29−80 years old) and 161 into the validation cohort (80 males and 81 females; median age 60 years old, range 29−81years old). The inclusion criteria were as follows, NSCLC confirmed by surgical pathology; availability of complete thin-slice (≤1 mm) chest images reconstructed with a standard algorithm in Digital Imaging and Communications in Medicine format within 1 month prior to surgery. The exclusion criteria were as follows, any treatment prior to surgery, marked image artifact and incomplete thin-slice images reconstructed with a standard algorithm in Digital Imaging and Communications in Medicine format. These cohorts were used to build the radiomics signatures. Then, among the whole population, patients were selected for further DM prognostic evaluation based on the following inclusion and exclusion criteria. Inclusion criteria were as follows: stage I NSCLC according to the eighth edition of the TNM classification for lung cancer by the International Association for the Study of Lung Cancer (4), follow-up period longer than 1 year if there was no DM. Exclusion criteria were as follows: any treatment between surgery date and follow-up ending, lost follow-up, combined with other malignancy, and nonlung cancer related death. Finally, 194 NSCLC patients (71 males and 123 females; median age 60 years old, range, 29−80 years old) with stage I were included for the study. The clinical data, including gender, age, T stage, overall stage, smoking history, serum carcinoembryonic antige (CEA) and histological types were obtained by reviewing the medical records. The study protocol was approved by the institutional review boards of the hospital. The need for informed patient consent was waived.

CT Scanning

All patients underwent scanning on a 256-slice CT scanner or 128-slice CT scanner (Brilliance-iCT and Ingenuity CT; Philips Healthcare). Breath-hold training was performed before each examination. All patients were asked to hold their breath at the end of inspiration. Unenhanced imaging was performed from the thoracic inlet to the middle portion of the kidneys. The following scanning parameters were used: slice thickness 1 mm; slice increment 1 mm; collimation 128 × 0.625 mm (iCT) or 64 × 0.625 mm (Ingenuity CT); rotation 0.5 seconds; pitch 0.8 (iCT) or 1.02 (Ingenuity CT); matrix 512 × 512; high and standard resolution algorithms; 120 kVp, and dose modulation ACS (iCT) or Z DOM (Ingenuity CT).

CT Morphology Evaluation

All the thin-slice CT images were interpreted by two thoracic radiologists (with 3 years and 13 years of experience in chest CT) who were blinded to each subject's identity and clinical data. Decisions on CT findings were reached by consensus. The maximum diameter, location, shape, density, interface, marginal characteristics, inner structures, adjacent structures, and pleural effusion were evaluated (12). The maximum diameter in the axial plane, which was automatically generated after segmentation, was used for the T staging. The location was classified as the peripheral or central. The shape of the lesion was classified as "irregular" or

"round/oval." Density was classified as solid or subsolid. The interfaces were classified into three types, that is, ill-defined, well-defined and smooth, and well-defined but coarse. Marginal characteristics included lobulation, spiculation, cusp angle, and spine-like process. Internal characteristics included cavity, vacuole sign, and air bronchograms. Air bronchograms were reclassified as natural, dilated/distorted, or cut-off. Findings in adjacent structures included the pleural thickening, pleural indentation sign, and vascular convergence sign.

Image Segmentation

The imaging segmentation methods used in the study were described in detail in the online supplementary material (https://doi.org/10.1007/s00330-018-5530-z) (13). The reproducibility of intraobserver and interobserver agreement of the features segmentation has been confirmed using inter-/intraclass correlation coefficients (ICCs) by two experienced thoracic radiologists with 3 years and 13 years of experience in our previous study (13).

Extraction and Selection of Radiomics Features and Building of the Radiomics Signature

The set of radiomics features used in this study contained 485 three-dimensional descriptors, which could be divided into shape features (n = 8), histogram features (n = 153), gray-level co-occurrence matrix features (n = 198), and gray-level run-length matrix features (n = 126). All the features were generated from the original CT image and eight kinds of filtered image except the shape features, which were generated from only the original image. The process of feature extraction was described in detail in **Supplementary material 1**. The feature extraction was performed in MATLAB 2014a (Mathworks, Natick, MA) using an in-house developed tool-box. Feature selection and radiomics signature building were based on the primary cohort. Firstly, ICCs were used to evaluate the intraobserver and interobserver agreement of the feature's extraction. An ICC >0.75 represents good agreement. Stable and reproducible features were normalized into a standardized value range by a z-score method and entered in the process of signature building. Then, we used the hierarchical clustering (14) with agglomerative ward linkage, a Pearson correlation-based dissimilarity measure and performed 10,000 resampling iterations (15). We selected the optimal cluster number that had the highest median cluster consensus to produce the largest intracluster consensus and the smallest intercluster ambiguity. The clusters were identified as radiomics signatures (RS). Finally, in order to estimate the RS types on each patient, two subtypes of patients (I or II type of each RS) were discovered using a further procedure of hierarchical clustering based on each RS.

Follow-up Procedure

Imaging examinations were used for the follow-up, the end point was defined as the detection of DM with CT, MRI, PET-CT or isotope bone scan, or confirmed `the DM by pathology. Once the DM was found, the follow-up would be ended; otherwise, the end date of follow-up is December 2017. These patients without DM until the end date of follow-up, were regarded as the censored data. The DM free survival (DMFS) was defined as the time from the priorsurgery CT examination date to the date of metastasis or end point of follow-up, which was expressed with months.

Statistical Analysis

The statistical analysis was performed using R software (version 3.0.1; R Foundation for Statistical Computing, Vienna, Austria; http://www.Rproject.org).The measurement data were expressed in median (range), classified variables were expressed in frequency and percentage. The intragroup proportions was used to test the similarity between radiomics signature classification and the feature clusters developed in the validation cohort. The hazard ratio (HR) of clinical features, CT morphological features and five radiomics signatures were calculated. The log-rank test was performed for the univariate survival analysis, then the multivariate survival analysis of Cox model was further performed to screen the independent prognostic factors. The "cutp" function of the "survMisc" R package, which had been proven to have good properties in the case of survival analysis with tied and censored data (16), was used to select the optimum cutoff for prognostic factors and Cox model to split patients into high-risk and low-risk groups. A two-sided p value <0.05 was considered statistically significant. Survival curve of each independent prognostic factor was drawn with Kaplan-Meier method. Harrell's concordance index (C-index), which measures the probability that the pairs of patients' predicted risks are correctly ordered (17,18), was also computed to quantify the prognostic performance. C-index = 0.5 indicates that the model is not better than random chance; the greater difference between the C-index and 0.5 indicates the better predictive performance.

RESULTS

Clinical Characteristic and Follow-up Results

The clinical characteristics including gender, age, T stage, overall stage, smoking history, serum CEA, and histological types were listed in Table 1. Until the follow-up end date, the median of follow-up duration was 21 months, ranged from 3 to 63 months. There were 25 patients (12.9%) with DM, including nine lung metastasis, six bone metastasis, four adrenal gland metastasis, two brain metastasis, one hepatic metastasis, one pleural metastasis, and two multiple organs metastasis. Eight patients (4.1%) died from lung cancer. The median DMFS was 15 months ranging from 3 to 54 months.

TABLE 1. Clinical Characteristics by the Univariate Survival Analysis in Stage I NSCLC

Characteristic	Overall (%)	Distant metastasis (%)	HR (95%CI)	C-index	*p* Value
Age*	60(29−80)	60(37−76)	1.002(0.966−1.039)	0.479(0.430−0.528)	0.255
Sex				0.566(0.475−0.657)	0.049
Male#	71(36.6)	13(18.3)	—		
Female	123(63.4)	12(9.8)	0.466(0.212−1.025)		
Smoking status				0.563(0.433−0.692)	0.286
Nonsmoker#	162(83.5)	19(11.7)	—		
Smoker	32(16.5)	6(18.8)	1.641(0.653−4.129)		
CEA(μg/L)				0.287(0.141−0.432)	0.007
≤5#	172(88.7)	17(9.9)	—		
5−20	22(11.3)	8(36.4)	3.097(1.325−7.239)		
>20	0(0.0)	0(0.0)	—		
T stage				0.437(0.369−0.504)	<0.001
T1a	26(13.4)	0(0.0)	—		
T1b	88(45.4)	5(5.7)	0.170(0.062−0.465)		
T1c	35(18.0)	4(11.4)	0.398(0.132−1.203)		
T2a#	45(23.2)	16(35.6)	—		
Overall stage				0.309(0.204−0.414)	<0.001
IA#	149(76.8)	9(6.0)	—		
IB	45(23.2)	16(35.6)	5.375(2.358−12.248)		
Histological type	0.123(0−0.305)	<0.001			
Adeno#	185(95.4)	18(9.7)	—		
Nonadeno	9(4.6)	7(77.8)	7.958(3.287−19.267)		

Note: —: None; Adeno, adenocarcinoma; Nonadeno, nonadenocarcinoma.

* Data in parentheses are the range.

In the calculation of HR, this is the reference group.

Selection of Radiomics Features and Building of the Radiomics Signature

Three hundred thirteen features with well reproducibility (ICC > 0.75) were selected. The consistent clustering analysis showed the optimal cluster number is five in the primary cohort. All the clusters in primary and validation cohort were robust with p <0.05 in the intragroup proportions statistic (Fig 1). The delta area plots, which depicts the relative increase in consensus when cluster number changing, are shown in **Supplementary Fig S1** (14). The radiomics features were then classified into five groups and labelled as radiomics signature 1 (RS1), RS2, RS3, RS4, and RS5. There were 112, 25, 50, 72, and 54 features in RS1, RS2, RS3, RS4, and RS5, respectively. The ten features with the highest average consensus indexes in each RS were listed in **Supplementary Table S1**. Subsequently, two subtypes of patients (I or II type of each RS) were discovered using a further procedure of hierarchical clustering based on each RS.

The Prognostic Value of Clinical Characteristics, CT Morphological Features and Radiomics Signatures

The univariate survival analysis was performed in clinical characteristics, CT morphological features and radiomics signatures, respectively, and revealed 20 predictors (5 clinical characteristics, 11 CT morphological features, and 4 radiomics signatures) were correlated to the DM. Table 1 showed the following five clinical characteristics: sex, CEA level, T stage, overall stage, and histological type were correlated with the DM ($p < 0.05$). The histological type exhibited a good prognostic ability with C-index of 0.123 (95% CI, 0.000−0.305; $p < 0.001$) for DMFS. Except for shape, lobulation, cusp angle, vacuole sign, and pleural thickening, other CT morphological features were the high-risk factors of postsurgical DM ($p < 0.05$, Table 2). The spiculation, pleural indentation, and pleural effusion showed relatively better prognostic ability for DMFS with C-index of 0.386 (95% CI, 0.297−0.475; $p < 0.001$), 0.505 (95% CI, 0.417−0.593; $p < 0.001$), and 0.304 (95% CI, 0.000−0.644; $p < 0.001$), respectively. All RSs have exactly two types (type I and type II). Significant difference was found between type I and type II in RS1, RS2, RS3, and RS5 for DMFS. Type II of RS1 and RS2, in comparison with type I, were the risk factors of DM (HR 29.714 and 3.777, respectively). In contrast, type II of RS3 and RS5 were the protective factors of DM (HR 0.242 and 0.365, respectively) in comparison with type I. The RS1 showed the best prognostic ability with C-index of 0.355(95% CI, 0.269−0.442; $p < 0.001$; Table 3). Furthermore, the prognostic performance of the 20 predictors were assessed by measuring how well they could distinguish patients with DM (**Supplementary Table S2**).

The Prognostic Value of Cox Model

The above mentioned 20 predictors were analyzed with Cox model, and found that histological type (HR 4.461, 95% CI

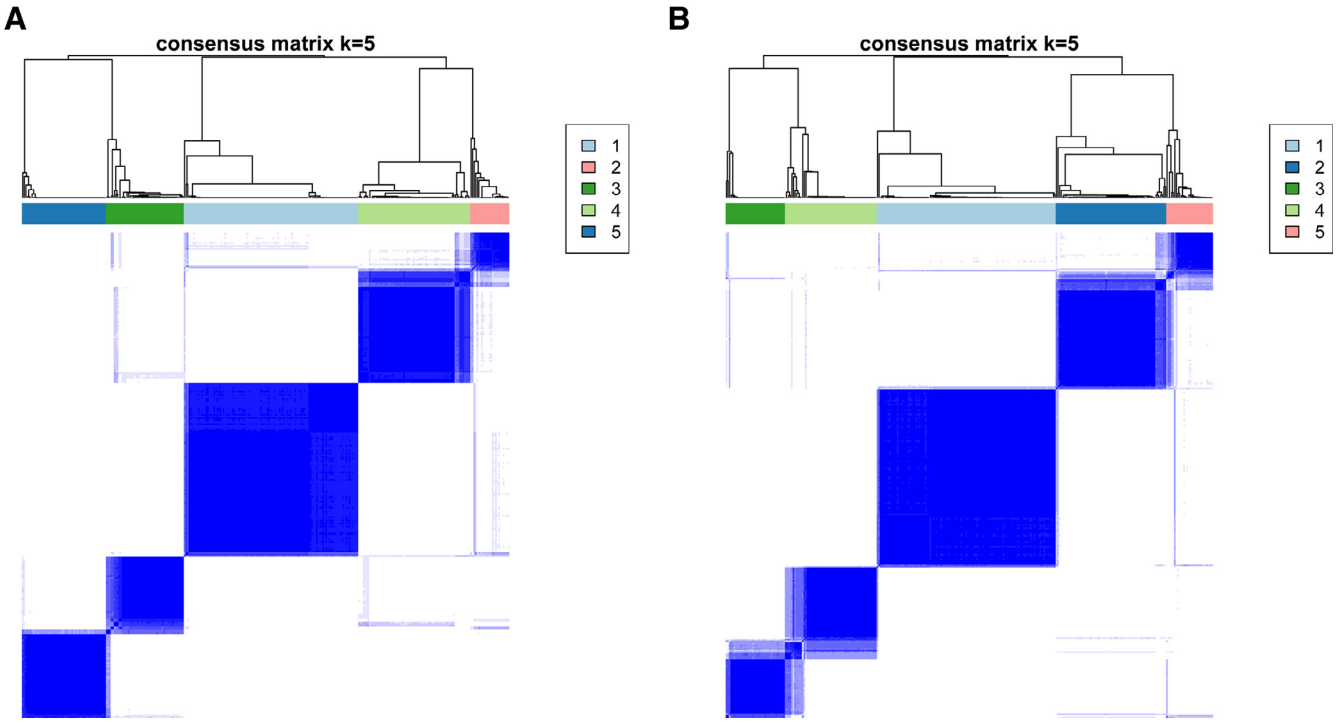

Figure 1. Consensus heatmaps for radiomics features ordered with respect to the obtained clusters. (A) The primary cohort; (B) the validation cohort. (Color version of figure is available online.)

1.783−11.162), pleural indentation sign (HR 2.623, 95% CI 1.070−6.426) and RS1 (HR 18.025, 95% CI 2.366−137.340) were the independent prognostic factors ($p < 0.05$, Table 4). Type II of RS1, pleural indentation sign and nonadenocarcinoma indicated the high probability of postsurgical DM. The Kaplan-Meier curves of high-risk and low-risk groups, which were spilt by Cox model and the optimum cutoff threshold, were statistically divergent (Fig 2) with sensitivity and specificity of 0.720 and 0.799 respectively. The C-index with Cox model was 0.407(95% CI, 0.344−0.470; $p < 0.001$).

DISCUSSION

About 30%−40% stage I NSCLC patients would have recurrence or DM postsurgery, the local recurrence rate of stage IA is 19% and the 5-year survival less than 80%, the stage IB with worse prognosis (2). The study evaluated the patients with postsurgery metastasis, and analyzed the feasibility of radiomics signature on the prediction of NSCLC prognosis. We built five radiomics signatures using consistent clustering analysis and found that RS1 showed the best prognostic ability. By combining radiomics features, CT morphological features and clinical characteristics, we found type II of RS1, pleural indentation sign and nonadenocarcinoma were the independent predictors of DM of stage I NSCLC.

The heterogeneity of biological behavior of tumor cells and gene usually indicates the worse prognosis. More heterogenous, more probable of drug resistance and DM. It has been reported that radiomics features could reflect the heterogeneity of tumor and predict the prognosis (19−21). In this study, unsupervised consensus clustering was used to establish radiomics signatures, which was different from prior studies with the least absolute shrinkage and selection operator logistic regression analysis (13). The radiomics signatures generated by consensus clustering could be regarded as an independent feature, just like the CT morphological features. Consensus clustering has been shown to be more robust and insensitive to random starts, and has been widely used to establish imaging subtypes of cancer, such as breast cancer and glioma (22,23). Coroller et al found that radiomic features could be used as a prognostic biomarker for clinically-relevant factors such as DM (24). In this study, five radiomics signatures were built using the similar consensus clustering method by Parmar (15) and RS1 was the independent predictor of DM of stage I NSCLC, with the highest HR (29.714, 95%CI 4.014−219.984, $p < 0.001$). The metastatic rate in type II of RS1 was significantly higher than that in type I (28.6% vs 0.9%, $p < 0.001$), respectively. Type II of RS1 was the high-risk factor of DM, suggesting the marked heterogeneity in the lung cancer with type II of RS1. Features extracted from the original image and the image filtered using a same filter (one of the low- and high-pass filters) along the x-, y-, and z-directions mainly composed the three most significant radiomics signatures RS1, RS2, and RS3. This implies that filtering isotopically might be a feasible preprocessing method for obtaining prognostic CT phenotype. RS1, which was found as an independent predictor of DM in our study, contained many histogram features and GLRLM features (Supplementary Table S1). Histogram features are

TABLE 2. CT Morphological Features by the Univariate Survival Analysis in Stage I NSCLC

Feature	Overall (%)	Distant Metastasis (%)	HR (95%CI)	C-index (95%CI)	*p* value
Maximum diameter*	1.8(0.6–4.7)	2.7(1.5–3.8)	2.077(1.426–3.024)	0.446(0.397–0.496)	<0.001
Location				0.354(0.046–0.662)	0.004
Central#	6(3.1)	3(50.0)	—		
Peripheral	188(96.9)	22(11.7)	0.193(0.057–0.650)		
Shape				0.573(0.474–0.672)	0.144
Irregular#	51(26.3)	4(7.8)	—		
Round	143(73.7)	21(14.7)	2.159(0.739–6.310)		
Density				0.400(0.330–0.467)	<0.001
Solid#	62(32.0)	22(35.5)	—		
Nonsolid	132(68.0)	3(2.3)	0.091(0.027–0.304)		
Interface				0.552(0.454–0.649)	0.021
ill-defined	5(2.6)	0(0.0)	—		
well defined and smooth	36(18.6)	0(0.0)	—		
well defined but coarse	153(78.9)	25(16.3)	—		
Lobulation (-)#	25(12.9)	1(4.0)	—	0.548(0.420–0.676)	0.130
Lobulation (+)	169(87.1)	24(14.2)	4.099(0.554–30.348)		
Spiculation (-)#	120(61.9)	7(5.8)	—	0.386(0.297–0.475)	<0.001
Spiculation (+)	74(38.1)	18(24.3)	4.027(1.679–9.661)		
Cusp angle (-)	188(96.9)	25(13.3)	—	0.612(0.391–0.833)	0.289
Cusp angle (+)	6(3.1)	0(0.0)	—		
Spine-like process (-)#	145(74.7)	13(9.0)	—	0.521(0.412–0.630)	0.002
Spine-like process (+)	49(25.3)	12(24.5)	3.361(1.508–7.491)		
Vacuole sign (-)#	100(51.5)	14(14.0)	—	0.443(0.357–0.529)	0.894
Vacuole sign (+)	94(48.5)	11(11.7)	0.922(0.418–2.037)		
Cavity sign (-)#	185(95.4)	22(11.9)	—	0.474(0.270–0.678)	0.030
Cavity sign (+)	9(4.6)	3(33.3)	3.567(1.062–11.989)		
Air bronchograms				0.534(0.453–0.616)	<0.001
None#	116(59.8)	10(8.6)	—		
Natural	31(16.0)	1(3.2)	0.277(0.035–2.169)		
Dilated/distorted	12(6.2)	1(8.3)	0.832(0.106–6.526)		
Cut-off	35(18.0)	13(37.1)	4.205(1.841–9.607)		
Pleural indentation (-)#	117(60.3)	9(7.7)	—	0.505(0.417–0.593)	0.003
Pleural indentation (+)	77(39.7)	16(20.8)	3.434(1.466–8.045)		
Thickened pleura (-)#	170(87.6)	22(12.9)	—	0.590(0.457–0.723)	0.989
Thickened pleura (+)	24(12.4)	3(12.5)	1.007(0.299–3.388)		
Pleural effusion (-)#	188(96.9)	21(11.2)	—	0.304(0–0.644)	<0.001
Pleural effusion (+)	6(3.1)	4(66.7)	7.449(2.530–21.931)		
Vascular convergence (-)#	135(69.6)	11(8.1)	—	0.464(0.360–0.567)	0.006
Vascular convergence (+)	59(30.4)	14(23.7)	2.924(1.321–6.470)		

Note: —: None.

* Data in parentheses are the range.

In the calculation of HR, this is the reference group.

able to reflect the distribution of image intensity level. For example, Uniformity trends to emphasize the even intensity distribution, while mass measures the tumor size and CT value simultaneously. GLRLM features quantify the heterogeneity of the tumor. Different from RS1, the most representative medoid features of RS2 and RS3 were almost all texture features, that is, GLCM features and GLRLM features, which might make the two signatures more sensitive to the local textural patterns rather than the low-level intensity characteristics. Fried et al found pretreatment tumor texture may provide prognostic information beyond what is obtained from conventional prognostic factors in stage III NSCLC (11). In comparison with most of the CT morphological features, RS showed better predictive performance, which was similar to the previous study. Balagurunathan et al evaluated the reproducibility and prognosis of CT quantitative features in 59 lung adenocarcinoma patients, extracting 219 features, and found run-length gray-level nonuniformity showed the optimal predictive performance with the AUC 0.93, accuracy 70.69%, sensitivity 47%, and specificity 96%, better than the traditional features, such as shape and size (25). In this study, the C-index of RS1 was 0.355 (95% CI, 0.269–0.442), better than that of shape 0.573 (95% CI, 0.474–0.672), and size 0.446 (95% CI, 0.397–0.496).

The pleural indentation sign was also a common and valuable indicator for differential diagnosis of malignancy. The

TABLE 3. Radiomics Signatures by the Univariate Survival Analysis in Stage I NSCLC

Radiomics Signature	Overall (%)	Distant Metastasis (%)	HR (95%CI)	C-index(95%CI)	*p* Value
RS1				0.355(0.369−0.442)	<0.001
Type I#	110(56.7)	1(0.9)	—		
Type II	84(43.3)	24(28.6)	29.714(4.014−219.984)		
RS2				0.571(0.462−0.681)	<0.001
Type I#	156(80.4)	15(9.6)	—		
Type II	38(19.6)	10(26.3)	3.777(1.666−8.560)		
RS3				0.481(0.374−0.587)	<0.001
Type I#	50(25.8)	14(28.0)	—		
Type II	144(74.2)	11(7.6)	0.242(0.110−0.535)		
RS4				0.445(0.355−0.535)	0.542
Type I#	119(61.3)	17(14.3)	—		
Type II	75(38.7)	8(10.7)	0.764(0.328−1.778)		
RS5				0.497(0.394−0.601)	0.011
Type I#	46(23.7)	11(23.9)	—		
Type II	148(76.3)	14(9.5)	0.365(0.165−0.807)		

Note: —: None.
In the calculation of HR, this is the reference group.

prerequisites of pleural indentation include the following two aspects: no conglutination between the parietal pleura and visceral pleura, and a distance between of lesion and pleura less than 2 cm (12). Based on these prerequisites, the contraction of fibrous tissue inside the lesion leads to pleural indentation. Pleural indentation sign is one of the important predictors for malignant lung nodule (12,26). In the present study, the metastatic rate in patients with pleural indentation was significantly higher than those without the pleural indentation (20.8% vs 7.7%, $p < 0.001$). Moreover, the Cox model showed pleural indentation was the independent predictor for the DM. Li et al found pit-fall sign on preoperative CT suggested a possible pleural involvement correlated with a poorer prognosis; the 5-year survival rate of pit-fall sign-positive patients was 46.5%, which was significantly lower than that of pit-fall sign-negative patients (68.9%; $p = 0.044$) (27). Lee found pleural indentation can differentiate the invasive adenocarcinoma from the noninvasive lesions (28). Therefore, the presence of pleural indentation suggested the more invasiveness and the more probability of DM.

The histological type was another independent predictor of DM for stage I NSCLC. However, the prognostic performance of histological type has not yet been reached consistent views. In this study, the adenocarcinoma accounted for 95.4% (185/194) and the postsurgery DM rate was 9.7% (18/185) lower than that in the nonadenocarcinoma 77.8% (7/9), indicating the nonadenocarcinoma with the poor prognosis. However, the sample size of nonadenocarcinoma was small and may draw a bias, more cases with nonadenocarcinoma should be included in the future. In contrast, Okada found the long-term prognosis of 5-year survivors with non-squamous cell carcinoma was worse (not significantly, $p = 0.0574$) than that of 5-year survivors with squamous cell carcinoma (29). The histopathologic difference in survival might suggest that in some cases adenocarcinoma could progress slowly and result in recurrence beyond 5 years after complete removal of the tumor.

This study has some limitations. First, it is of retrospective and potential bias, especially for the small sample size of nonadenocarcinoma, the predictive performance of histological type would be affected. More nonadenocarcinoma cases should be included in the future to draw more accurate results. Second, the median follow-up period was 21 months, which was relatively short, and some cases have not yet reached the end event point, the longer follow-up should be performed for the stage I NSCLC in the future. Third, radiomics features were derived from the results of manual segmentation. Small internal vessels and the bronchi could not be excluded, which would have affected the accuracy of some features. Therefore, a reliable and robust automatic boundary extraction method needs to be used.

In conclusion, radiomics provided a new modality for the distant metastatic prediction of stage I NSCLC. The RS1, pleural indentation sign and histological type were the independent predictors of DM. Patients with type II of RS1,

TABLE 4. Risk Factors for Distant Metastasis in Stage I NSCLC With Multivariate Cox Regression

Prognostic factor	β	Adjusted HR	95%CI	*p* Value
RS1 (type II vs type I)	2.892	18.025	2.366−137.340	0.005
Pleural indentation (with vs without)	0.964	2.623	1.070−6.426	0.035
Histological subtype (Nonadeno vs adeno)	1.496	4.461	1.783−11.162	0.001

Note: β, multivariate Cox regression coefficient; Adeno, adenocarcinomas; Nonadeno, nonadenocarcinoma.

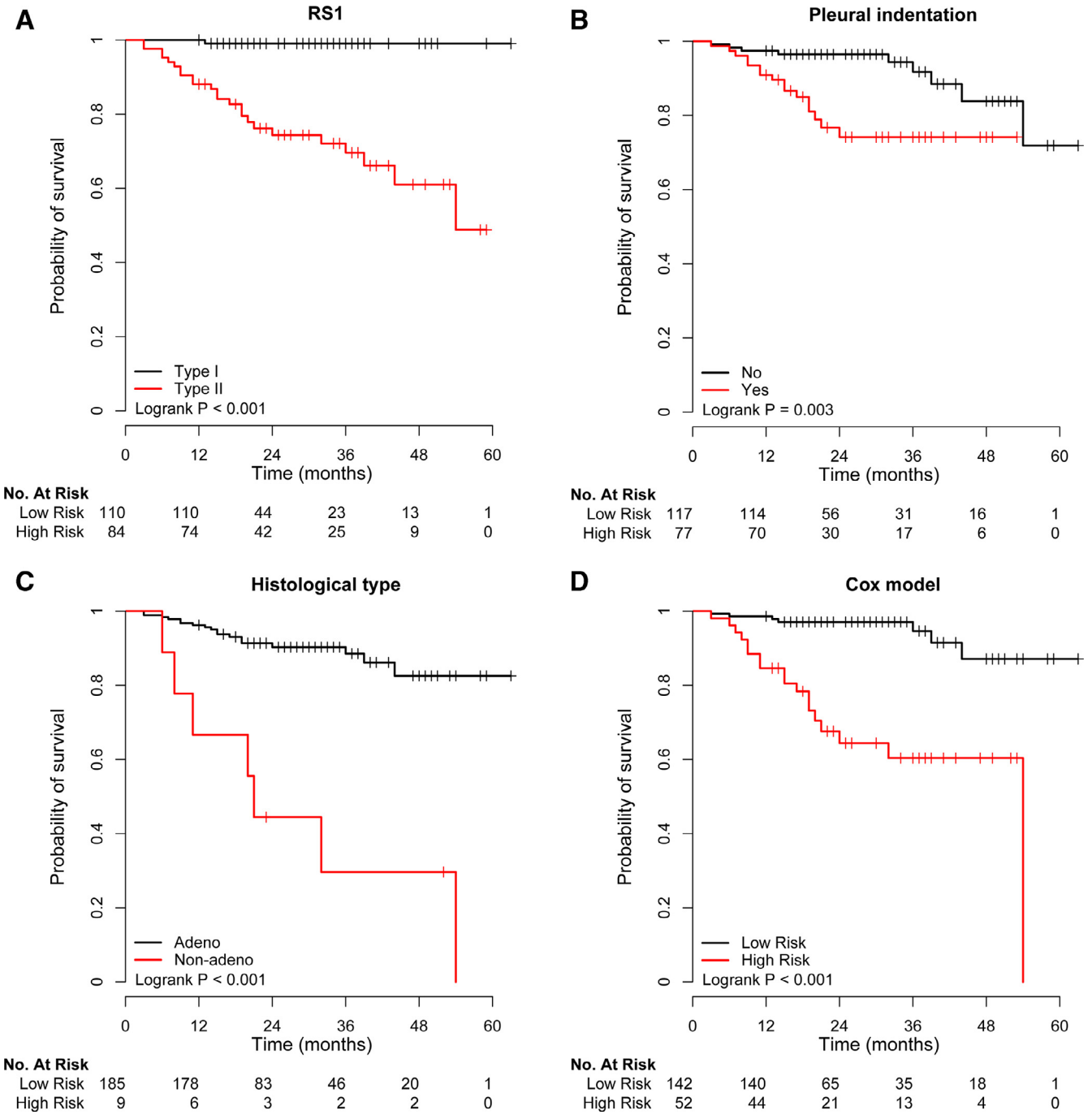

Figure 2. Survival curve of RS1, pleural indentation sign and histological type in 194 NSCLC patients. (A) Type II vs. type I of RS1; (B) with pleural indentation sign vs without pleural indentation sign; (C) Adenocarcinoma vs non-adenocarcinoma; (D) high-risk vs low-risk split by Cox model. (Color version of figure is available online.)

pleural indentation sign and nonadenocarcinoma indicating the high probability of postsurgical DM, are recommended to receive the adjuvant therapy postsurgery.

FUNDING

This work was supported by the National Key R&D Program of China (grant numbers 2016YFE0103000 and 2017YFC1308703); the National Natural Science Foundation of China (grant numbers 81871321 and 81370035), the Youth Fund of the National Natural Science Foundation of China (grant number 81501618).

SUPPLEMENTARY MATERIALS

Supplementary material associated with this article can be found in the online version at doi:10.1016/j.acra.2018.11.004.

REFERENCES

1. Chansky K, Detterbeck FC, Nicholson AG, et al. The IASLC lung cancer staging project: external validation of the revision of the TNM stage groupings in the eighth edition of the TNM classification of lung cancer. J Thorac Oncol 2017; 12:1109–1121.
2. Fedor D, Johnson WR, Singhal S. Local recurrence following lung cancer surgery: incidence, risk factors, and outcomes. Surg Oncol 2013; 22:156–161.
3. Gibson AJW, Li H, D'Silva A, Tudor RA, et al. Comparison of clinical characteristics and outcomes in relapsed versus de novo metastatic non-small cell lung cancer. Am J Clin Oncol 2018. doi:10.1097/COC.0000000000000483.
4. Goldstraw P, Chansky K, Crowley J, et al. The IASLC lung cancer staging project: proposals for revision of the TNM stage groupings in the forthcoming (Eighth) edition of the TNM classification for lung cancer. J Thorac Oncol 2016; 11:39–51.
5. Chiappetta M, Leuzzi G, Sperduti I, et al. Lymph-node ratio predicts survival among the different stages of non-small-cell lung cancer: a multicentre analysis. Eur J Cardiothorac Surg 2018. doi:10.1093/ejcts/ezy311.
6. Lee J, Li B, Cui Y, et al. A quantitative CT imaging signature predicts survival and complements established prognosticators in stage I non-small cell lung cancer. Int J Radiat Oncol Biol Phys 2018. doi:10.1016/j.ijrobp.2018.01.006. pii: S0360-3016(18)30006-3.
7. Virginia BM, Laura F, Silvia R, et al. Prognostic value of histogram analysis in advanced non-small cell lung cancer: a radiomic study. Oncotarget 2017; 9:1906–1914.
8. Aktas GE, Karamustafaoğlu YA, Balta C, et al. Prognostic significance of fluorine-18 fluorodeoxyglucose positron emission tomography/computed tomography-derived metabolic parameters in surgically resected clinical-N0 nonsmall cell lung cancer. Nucl Med Commun. 2018. doi:10.1097/MNM.0000000000000903.
9. Aerts HJ, Velazquez ER, Leijenaar RT, et al. Decoding tumour phenotype by noninvasive imaging using a quantitative radiomics approach. Nat Commun 2014; 5:4006.
10. Li J, Fang M, Wang R, et al. Diagnostic accuracy of dual-energy CT-based nomograms to predict lymph node metastasis in gastric cancer. Eur Radiol 2018. doi:10.1007/s00330-018-5483-2.
11. Fried DV, Tucker SL, Zhou S, et al. Prognostic value and reproducibility of pretreatment CT texture features in stage III non-small cell lung cancer. Int J Radiat Oncol Biol Phys 2014; 90:834–842.
12. Fan L, Liu SY, Li QC, et al. Multidetector CT features of pulmonary focal ground-glass opacity: differences between benign and malignant. Br J Radiol 2012; 85:897–904.
13. Fan L, Fang M, Li Z, et al. Radiomics signature: a biomarker for the preoperative discrimination of lung invasive adenocarcinoma manifesting as a ground-glass nodule. Eur Radiol 2018. doi:10.1007/s00330-018-5530-z.
14. Monti S, Tamayo P, Mesirov J, et al. Consensus clustering: a resampling-based method for class discovery and visualization of gene expression microarray data. Machine learning 2003; 52:91–118.
15. Parmar C, Leijenaar RT, Grossmann P, et al. Radiomic feature clusters and prognostic signatures specific for Lung and Head & Neck cancer. Sci Rep 2015; 5:11044.
16. Choi YS, Ahn SS, Kim DW, et al. Incremental prognostic value of ADC histogram analysis over MGMT promoter methylation status in patients with glioblastoma. Radiology 2016; 281:175–184.
17. Koziol JA, Jia Z. The concordance index C and the Mann-Whitney parameter Pr(X > Y) with randomly censored data. Biom J 2009; 51:467–474.
18. Harrell Jr FE, Lee KL, Mark DB. Multivariable prognostic models: issues in developing models, evaluating assumptions and adequacy, and measuring and reducing errors. Stat Med 1996; 15:361–387.
19. Lambin P, Rios-Velazquez E, Leijenaar R, et al. Radiomics: extracting more information from medical images using advanced feature analysis. Eur J Cancer 2012; 48:441–446.
20. Ganeshan B, Panayiotou E, Burnand K, et al. Tumour heterogeneity in non-small cell lung carcinoma assessed by CT texture analysis: a potential marker of survival. Eur Radiol 2012; 22:796–802.
21. Chicklore S, Goh V, Siddique M, et al. Quantifying tumour heterogeneity in 18F-FDG PET/CT imaging by texture analysis. Eur J Nucl Med Mol Imaging 2013; 40:133–140.
22. Wu J, Cui Y, Sun X, et al. Unsupervised clustering of quantitative image phenotypes reveals breast cancer subtypes with distinct prognoses and molecular pathways. Clin Cancer Res 2017; 23:3334–3342.
23. Itakura H, Achrol AS, Mitchell LA, et al. Magnetic resonance image features identify glioblastoma phenotypic subtypes with distinct molecular pathway activities. Sci Transl Med 2015; 7. 303ra138.
24. Coroller TP, Grossmann P, Hou Y, et al. CT-based radiomic signature predicts distant metastasis in lung adenocarcinoma. Radiother Oncol 2015; 114:345–350.
25. Balagurunathan Y, Gu Y, Wang H, et al. Reproducibility and prognosis of quantitative features extracted from CT images. Transl Oncol 2014; 7:72–87.
26. Fan L, Liu SY, Li QC, et al. Pulmonary malignant focal ground-glass opacity nodules and solid nodules of 3cm or less: comparison of multidetector CT features. J Med Imaging Radiat Oncol 2011; 55:279–285.
27. Li M, Ito H, Wada H, et al. Pit-fall sign on computed tomography predicts pleural involvement and poor prognosis in non-small cell lung cancer. Lung Cancer 2004; 46:349–355.
28. Lee SM, Park CM, Goo JM, et al. Invasive pulmonary adenocarcinomas versus preinvasive lesions appearing as ground-glass nodules: differentiation by using CT features. Radiology 2013; 268:265–273.
29. Okada M, Nishio W, Sakamoto T, et al. Long-term survival and prognostic factors of five-year survivors with complete resection of non-small cell lung carcinoma. J Thorac Cardiovasc Surg 2003; 126:558–562.